DOI: 10.61782/fa.2023.0316

forum acusticum 2023

IMPROVEMENT OF FUSELAGE PERFORMANCE USING COUPLED CMA-ES OPTIMIZATION ALGORITHM AND CURVED TMM

François-Xavier Bécot*, **Luc Jaouen, Fabien Chevillotte**
MATELYS – Research Lab
7 rue des Maraîchers, Bât B, 69120 Vaulx-en-Velin, France

ABSTRACT

For aircraft propulsion, Distributed Electric Propulsion (DEP) consisting of a series of smaller propellers distributed over the wing, appears as a credible alternative to single large propeller system. However, they generate annoying mid and high frequency noise in addition to the classical blade passing frequency (BPF). The overall goal of the SILENTPROP EU project is to understand this interaction and by using advanced modeling techniques, to control the exterior and fuselage interior sound. The work presented here focuses on drawing some guidelines to the design of a fuselage trim adapted to DEP. For this a Transfer Matrix Solver (TMM) solver developed for curved structures is coupled to a Covariance matrix adaptation evolution strategy (CMA-ES) algorithm. The TMM model enables to represent different air-borne and structure-borne excitations. It also enables to consider complex fuselage structure including poroelastic trims, possibly with embedded resonators or materials featuring multi-scale phenomena. CMA-ES is a powerful approach known for its powerful global optimization capabilities. Results are presented here for a series of baseline designs and optimizing the trim composition for diffuse sound field excitation only. It is shown that a significant noise reduction improvement can be achieved at both BPF and mid to high frequency by a careful tuning of the fuselage composition.

Keywords: TMM, CMAES, porous, aircraft.

1. INTRODUCTION

With the rapid increase of costs of the fossil energy, electric propulsion has become a tangible alternative to pure internal combustion engine. For aircraft development, this fosters the development of alternative propulsion architecture like Distributed Electric Propulsion. The principle of DEP is to replace large jet engine or large propeller system by a series of smaller propellers distributed over the wing, see Figure 1.

Figure 1: Example of Distributed Electric Propulsion concepts. Extract from [1].

This was proved to be relevant in many aspects: it distributes the lift forces over the entire wing, thereby making the propulsion more efficient and relaxing mechanical

*Corresponding author: fxb@matelys.com.

constraints. It rises however several challenges in terms of acoustics. In addition to the classical blade passing frequency (BPF), DEP uses high speed rotation engines which create higher pitch broad band noise, known to be more disturbing, see for instance Figure 2. In addition, the aero-acoustic interaction between adjacent propellers may lead to increasing the overall noise in some regions of space. Whereas the direction towards the ground could be tapered, the sound may be redirected towards the fuselage, yielding a possible degradation of the cabin interior acoustic field.

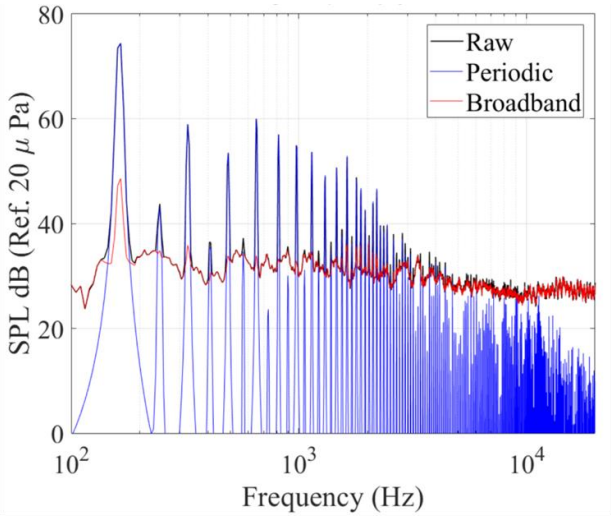

Figure 2: Example of contributions from tonal (*Periodic*), *Broadband* noise to tonal noise (*Raw*). Measured data from [2].

On the other hand, optimization techniques have grown a significant interest in the recent years, thanks to a wide spread of large computation resources. A very active field in this domain concerns the topology optimization, in particular for structural purposes. One of the widely used algorithm is called CMA-ES for Covariance Matrix Adaptation with Evolution Strategy [3]. This algorithm is not problem specific and is known to outperform other fundamental methods at high computational budget. This method falls into meta-heuristics, meaning that it is a heuristic of a heuristic method. Whereas heuristic methods may find local minimum in a large candidate space by successive iterations for improving the solution, meta-heuristic methods guide the search process to improve the convergence rate towards a global solution and to avoid being trapped in a local minimum. A good review of meta-heuristic methods may be found in [4]. In addition, *Evolution Strategy*, like genetic algorithm, means that the method is derivative- or gradient-free. This implies that only function evaluations are used and the objective function to be optimized needs not to be known explicitly. It also implies that the search relies on results obtained across a population of results, by opposition of trajectory-based methods which try to establish a link between the successive results to improve the convergence rate.

In general, CMA-ES is known to be well adapted to optimization problem with multiple variables, which may be the case of our concern here. Finally, one should note that this algorithm is a *stochastic* method, implying that the result may differ for the same initial guess. Therefore, several realizations of the same search may be necessary to provide sufficient representative statistics [5].

This paper first presents the solver used to compute the objective function. It is based on the Transfer Matrix Method (TMM) for curved geometries. Then, the coupling between CMA-ES and the solver together with the definition of the objective function is described. In the last section, a series of optimization problems are presented so as to discuss the ability of designing optimal properties of the trim to sound proof the fuselage envelope submitted to propeller noise.

2. MODELLING APPROACH

2.1 Transfer Matrix method

In the present work, simulation results are computed using the Transfer Matrix Method, also known as TMM [6]. More specifically, the *AlphaCell* software product [7] is used which implements the method proposed in [8] to improve the numerical stability of the computation.

Generally speaking, TMM is a powerful modelling scheme to solve complex problems involving a large variety of materials: solids, may they be isotropic or orthotropic, poro-elastic materials, heterogeneous media (materials with porous or solid inclusions, resonators, compressed materials, …), (micro-)perforated plates, laminate composites etc. In addition, these media may exhibit frequency varying properties. The response can be obtained for a variety of excitations, typically plane waves, diffuse sound field, mechanical force, rain fall, tapping machine, turbulent boundary layer… At each considered frequency, all relevant wave numbers (compression, bending, shear) are computed for each layer of the model. The continuity of pressure and displacement at each interface is then ensured and the response of the entire multi-layer system is solved.

It is finally worth noting that numerous works proposed to increase the modelling capacity using TMM, like taking into account the lateral size of the sample. Interested readers are referred to the dedicated chapter in the newest edition of

Allard's book about sound propagation in porous media [9]. One of them is the possibility to model curved structures. This feature is used in the present work and further discussed in the following.

2.2 TMM for curved geometries

In order to better cope with the actual fuselage geometry, a TMM model for curved structures is considered here. This model is also implemented in the *AlphaCell* software product after the works presented in [10], [11].
Curved geometries may be represented with the same complexity as for flat structure, namely including orthotropic plates and shells, poro-elastic materials, heterogeneities etc. In addition to the critical frequency observed for a system having a flat geometry, the cylindrical system will exhibit a so-called ring frequency, which is defined for a single homogeneous layer as one compressional wavelength fitting the perimeter of the cylinder:

$$f_{ring} = \frac{\sqrt{E/\rho}}{2\pi R_{cyl}}$$

where E and ρ are the Young's modulus and the mass density of the material and R_{cyl} is the radius of the cylinder. These two frequencies will correspond to two minima of the sound transmission loss (STL).

2.3 Application to fuselage STL prediction

In the present study, the fuselage is modelled as an infinitely long cylinder excited by an external diffuse sound field (see Figure 3). The outer radius of curvature is set to the order of magnitude of a typical passenger aircraft, namely 2 meters. The entire fuselage envelope comprises a 3 mm aluminum outer skin and a 4 mm plastic trim interior panel. Two air gaps dimensions are examined: either 42 or 22 mm. This space is partially filled with either a 20 mm or a 40 mm thick glasswool mat, leaving two 1 mm air gaps on each side to ensure a full decoupling with the inner and outer fuselage skin. A low density glasswool is supposed here, namely having 10 kg/m^3. This justifies the use of the *Limp* assumption against a full poro-elastic model which would more computationally demanding. It is finally assumed that such low density glasswool can be accurately represented using the Delany-Bazley-Miki model, which requires a single input parameter, the static air flow resistivity.

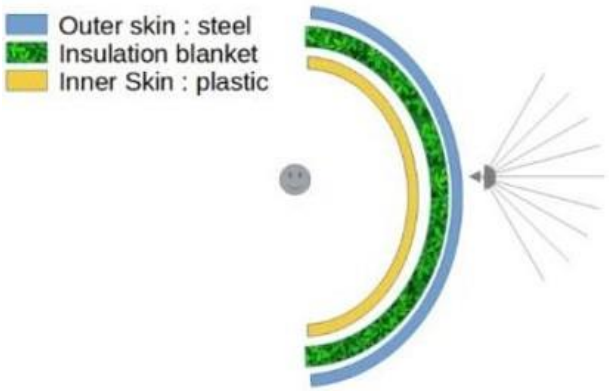

Figure 3: Composition of the base configuration of the cylindrical fuselage.

The typical response of the base fuselage configuration (see system depicted in Figure 3) is shown in Figure 4 below where the response for a similar flat structure is also shown. Comparing these two STL shows that the critical frequency is observed at the same position for both geometries. However, at lower frequencies, the flat system only exhibits the mass-spring-mass resonance around 220 Hz. To the contrary, in addition to this resonance, results for the curved geometry exhibit the ring frequency at 430 Hz, as theoretically estimated for the aluminum shell alone.

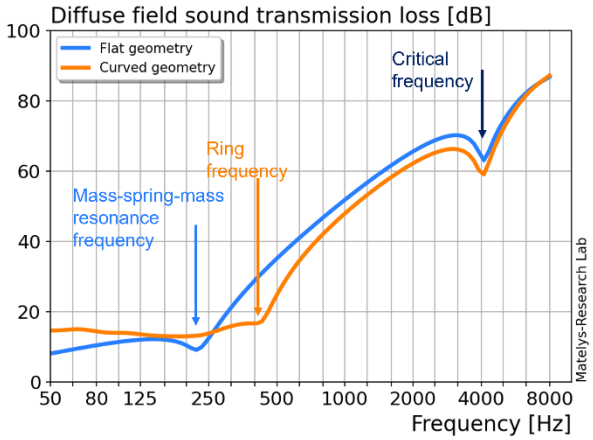

Figure 4: Sound transmission loss of the base fuselage configuration with air gap of 22 mm.

One should also highlight that STL levels at very low frequencies, namely below the first system resonance, are higher for the curved geometry than for the flat one. At these frequencies, the STL is mainly driven by the stiffness of the system due to boundary conditions. From a modeling point

of view, the curved configuration exhibits a higher stiffness than that of the flat plate which is assumed to be of infinite extent.
Note also that the spatial windowing, see for instance [12], is not able to correct this effect as it corresponds to a correction of the sound radiation efficiency. In other words, it does account for the actual boundary conditions (simply supported, clamped, …) and a possible modal behavior cannot be represented in this model.
Considering that the BPF occurs typically in the interval [100-200] Hz, these results finally foster the importance of an accurate design of the fuselage performance at these frequencies.

3. SETTING OF THE OPTIMIZATION ALGORITHM

3.1 Optimization algorithm and penalty functions

The TMM solver as described above for curved structure is coupled to a CMA-ES algorithm via the computation of a specific objective function.
The CMA-ES implementation is inspired from the source code package by Hansen [13]. Default parameter values are used here for the population size and number of parents. The maximum number of iterations allowed to reach convergence before ending the process anyway is set to 100.
The CMA-ES algorithm is set to minimize the objective function defined as the average of the transmission coefficient τ over a given frequency range:

$$objective \quad = Min(<\tau(f)>_{f_{range}})$$

where $\tau = 10^{-STL/10}$ and STL is the sound transmission loss expressed in decibels.
The aim of the optimization is to maximize the STL levels on a frequency range as low as possible, typically below 1000 Hz, and possibly including the BPF. In order to give more strength to the low frequency points, which are known to correspond to the weakest level of performance of the envelope, the average is calculated using two different penalty functions.
The first possible average is carried out only for frequency points below 500 Hz. This refers to as *Narrow freq.* penalty in the following. A second option consists in penalizing the transmission coefficients with weights between 1 and 10 linearly spaced in the frequency range below 500 Hz. This is intended to increase the weight of the BPF region. This penalty function is referred to as *Lin. penalty*. Optimization results obtained for these two types of averages are compared in the next section. Note finally that other forms of penalty are currently under examination, like a Gauss-like function centered around the BPF with a given frequency band width.

3.2 Optimization design variables

As mentioned above, the thermo-acoustic blanket is represented using a Delany-Bazley-Miki model under the *Limp* assumption. It is chosen here to fix the mass density and let only the air flow resistivity vary. It is indeed assumed that the mass density has little influence on the STL values for the arrangement chosen here.
However, it is well known that these porous materials have low efficiency at low frequency. Therefore, in order to maximize the acoustic efficiency of the blanket in the BPF range, resonators are embedded into the glasswool. The expected behavior is illustrated in Figure 5 the below, which shows the sound absorption of this arrangement glasswool + resonators. It is clearly seen that the resonators provide a significant gain at their tuned resonance frequencies and only in this narrow frequency band. Embedding them in the glasswool enables to retrieve the mid and high frequency range sound absorption brought by the porous material. It can finally be observed that the level may decrease at higher frequencies, here above 2 500 Hz, due to an additional tortuosity effect brought by the presence of the resonators. This effect tends to increase the reflexion of the incident sound waves, thus decreasing the sound absorption.

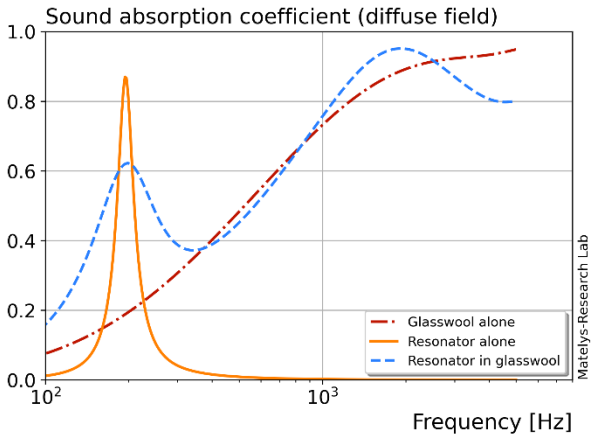

Figure 5 : Sound absorption coefficient in diffuse field for a blanket having 40 mm thick and resonators tuned at 201 Hz, filling the volume at 50%.

In the present study, resonators are supposed to follow a similar construction principle as those studied theoretically

and experimentally in [14], [15] , as depicted in Figure 6. Namely, the resonator neck length is set according to the cavity size, either equal to the radius or to the diameter. It is further assumed that the volume of the cavity is not affected by the volume of the neck. This construction, without being restrictive, has the advantage of reducing the number of degrees of freedom of the design.

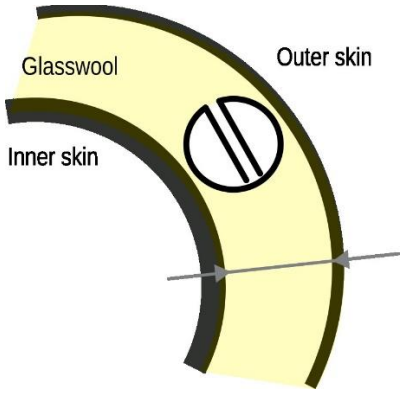

Figure 6 : Scheme of air-borne resonators embedded into the fuselage insulation blanket.

As a result, two-variable optimizations are carried out : one variable being related to the blanket, the air flow resistivity, and another being related to the resonator. Optimization results are presented in the next section.

4. OPTIMIZATION RESULTS

This section presents optimization results obtained for resonators tuned at around either 800 Hz or 200 Hz. These frequencies correspond to the BPF of, respectively an 8-blade or a 2-blade propeller rotating at 6000 revolutions per minute (RPM).
Results are shown for optimization of the cavity radius in paragraph 4.1 and for the optimization of the rate of the inclusion of the resonator, i.e. the number of resonators per unit volume in paragraph 4.2. For each case, the results, assessed in terms of STL, are compared with the performance of the base configuration having the glasswool without resonators. In order to help the result interpretation, the power dissipated within the glasswool blanket without and with the resonators are also shown to assess the gain brought by the presence of the resonators.

4.1 Air flow resistivity and cavity radius

In this section, the optimization process concerns the air flow resistivity of the blanket and the resonator cavity radius. The air space between the outer and inner material is set to 20 mm. Thus, the maximum allowed value for the cavity radius is set to 20 mm. A 20 mm thick blanket is assumed to embed resonators with a 24% rate of inclusion. The resonator neck radius is fixed to 2 mm. The neck length is set to be equal to the cavity radius. Results are shown in **Erreur ! Source du renvoi introuvable.**.

	Air flow resistivity [N.s.m^{-4}]	Cavity radius [mm]	Resonator frequency [Hz]
No penalty	10 000	19.2	240
Lin. penalty	9 999	10.3	801
Freq. < 500 Hz	9 999	18.2	264

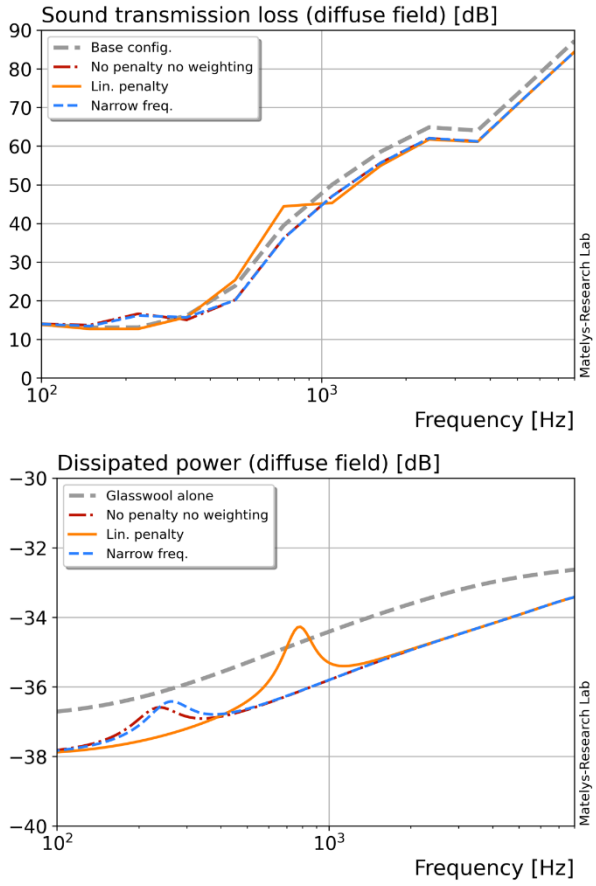

Figure 7 : Optimization of the fuselage STL for glasswool air flow resistivity and resonator cavity radius. Fuselage 2 m curvature radius ; blanket 20 mm thick ; resonators: 24% of inclusion, cavity radius equal to neck length.

It is observed that simulations obtained with no penalty enable to increase the STL values at low frequencies. This corresponds indeed to the frequency region of less efficiency of the base configuration, which, as a reminder, corresponds to both the mass-spring-mass resonance frequency of the fuselage envelope and to the BPF. The obtained resonator radius leads to having a resonance frequency at 240 Hz. The improvement, about 5 dB, is clear at this particular frequency. This is however followed by a decrease of the STL levels for frequencies above 400 Hz compared to the blanket without resonators.
The strategy considering only frequencies below 500 Hz (*Narrow freq.*) gives results which are very similar to those obtained without penalty. The optimal resonator is indeed tuned at 264 Hz here, which is close to the 240 Hz above. The strategy with linear penalty yields an optimized resonator tuned at 801 Hz. As a result, similar results as the configuration without resonators are obtained at frequencies below 400 Hz and a clear gain is observed around 800 Hz. The increase reaches 5 dB at this frequency, confirming the efficiency of the tuned resonator. At higher frequencies, STL levels tend to those obtained using the other objective functions.
At frequencies above 400 Hz, all configurations with resonators show STL values which are 3 dB lower than the base configuration without resonators. This is due to the increase of the compressibility of the air space due to the resonators, which is a known phenomenon for tuned resonating systems. Furthermore, the presence of the resonators may decrease the porous volume available for dissipating the acoustic energy, as clearly seen on the graph of the dissipated powers, see **Erreur ! Source du renvoi introuvable.**-bottom insert. This loss of dissipation capacity is not compensated by the additional dissipation brought by the resonators. It is indeed only compensated for in the limited frequency ranges of the resonator resonances.
One can also notice that the overall dissipated power for the glasswool with resonators is lower than that without resonators. This level is globally the same for all optimization strategies, except at the resonance frequencies of the resonators. This is mainly due to the fact that the rate of inclusion is kept constant for all strategies. It should be noted that the STL of the system with resonators may exceed that of the system without resonators even if the dissipated power in the blanket diminishes compared to the base configuration without resonators. This is observed around 200 Hz. This means that besides the visco-thermal dissipation, the resonators also block the sound to be transmitted through the blanket.
Concerning the blanket, none of the optimization algorithm manages to adjust the glasswool properties to compensate the loss of dissipation due to the presence of the resonators. All strategies give similar values of the air flow resistivity, which is close to the initial value of 10 000 N.s.m^{-4}. This means that this value is already close to the optimal one.
In total, the gain brought by the resonators is clearly seen at low frequencies but to the expense of high frequency performance. It is also interesting to see that a certain tolerance may be given to the tuning of the resonator resonance frequency while achieving similar performance in a given frequency range.

4.2 Air flow resistivity and resonator rate of inclusion

The second illustration example considers as optimization variables the blanket air flow resistivity and the rate of inclusion of the resonators. The blanket is now having 40 mm thickness. The resonators, which radius are set to the blanket thickness, are now tuned exactly at the BPF of 2 blades' propeller rotating at 6 000 RPM, i.e. 201 Hz. Results of the optimization are presented similarly as above, in **Erreur ! Source du renvoi introuvable.**.
As in the previous example, the strategy with no penalty yields improved STL levels around its weakest point, namely below 250 Hz. Compared to the base configuration, the gain reaches 7 dB at 150 Hz. At higher frequencies though, the obtained STL values are lower by about 15 dB, due to a high rate of inclusion, over 70 % in this case.
It is also observed that the strategy using the linear penalty gives results, which are similar to those of the base configuration without resonator. Indeed, the optimal inclusion rate in this case is obtained at 1 %, which does not provide a sufficient number of resonators for their effect to be visible.
The final strategy giving emphasis to frequencies below 500 Hz gives similar results as the strategy with no penalties up to 500 Hz, namely providing a 7 dB gain at the BPF. At higher frequencies, the decrease in STL values is limited to 10 dB, which may still be prohibitive in a real application but represents a compromise between the two other optimization results. The algorithm predicts a rate of inclusion of 59 %, which seems to be a compromise between increased performance at low frequencies and as moderate decrease as possible at higher frequencies.
The dissipated powers (see Figure 8-bottom insert) closely follow the aforementioned tendencies for all strategies. As already illustrated by the previous example, the dissipated power levels are not fully correlated with the STL levels. It is observed for frequencies below 800 Hz, that the STL levels could be both lower, respectively higher, than the base configuration without resonators, while the dissipated power

of the configuration with resonators always exceeds that of the base configuration without resonators. As explained above, this is due the presence of the resonators blocking the sound waves, thus increasing the sound reflexion, rather than dissipating the sound energy.
Finally, as expected in the view of the results of the first example, the optimal values are all obtained about 10 000 N.s.m^{-4}. This confirms that the initial value of the blanket air flow resistivity seems may be close to the optimal.

	Air flow resistivity [N.s.m^{-4}]	Inclusion rate [%]	Resonator frequency [Hz]
No penalty	10 000	70.9	201
Lin. penalty	9 999	1.0	201
Freq. < 500 Hz	10 000	58.7	201

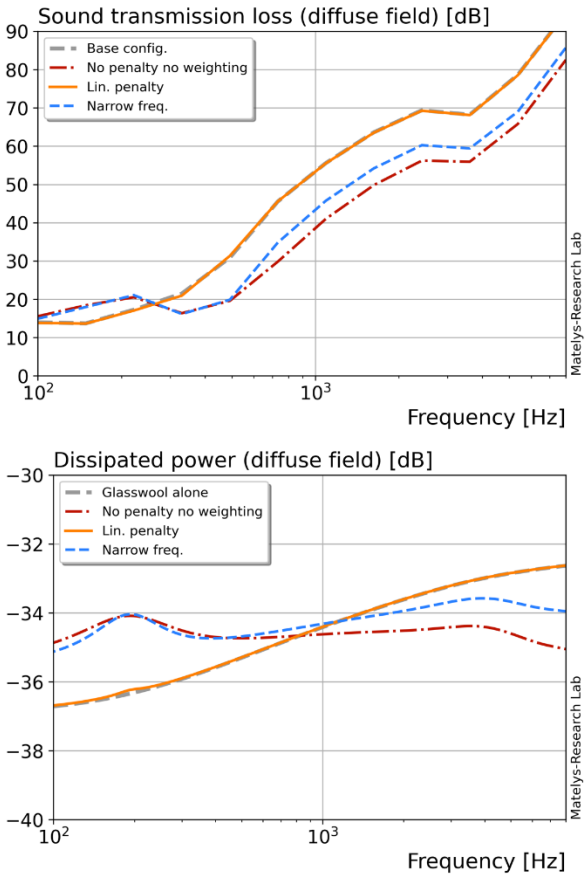

Figure 8 : Optimization of the fuselage STL for glasswool air flow resistivity and resonator rate of inclusion. Fuselage 2 m curvature radius ; blanket 40 mm thick ; resonators tuned at 201 Hz.

5. CONCLUDING REMARKS

The present work aims at examining the use of a state-of-the-art algorithm to optimize the sound insulation performance of a fuselage submitted to air-borne sound excitation. The prediction core is based on a TMM solver for curved structures and is coupled to a CMA-ES optimization algorithm. The fuselage system is represented by an outer aluminum shell and an inner plastic trim. The intermediate thermo-acoustic blanket is chosen to be a glasswool with embedded Helmholtz resonators. The optimized parameters are set to be the air flow resistivity of the glasswool and the dimensions or the number of resonators per unit volume. The above seminal results show that the optimization algorithm could help reaching a compromise between low and high frequency performance. Work is currently undergoing to improve the penalty function to improve accounting for the system response at the BPF. Also, efforts are made to include more variable parameters, such as the weight of elements (blanket, fuselage envelope) and to include a finer design of the porous material micro-structure, possibly using heterogeneities (double porosity, porous composite, sorption effects) to activate multiple scale or additional physical effects.

6. ACKNOWLEDGMENTS

This work is carried out in the framework of the European research project SILENTPROP, which is financially supported by the CLEANSKY 2 programme, agreement 882842. The project partners are also greatly acknowledged : Univ. of Nottingham (UK), Univ. of Bristol (UK), Mejzlik (CZ).

7. REFERENCES

[1] H. D. Kim, A. T. Perry, and P. J. Ansell, "A Review of Distributed Electric Propulsion Concepts for Air Vehicle Technology," in *2018 AIAA/IEEE Electric Aircraft Technologies Symposium*, Cincinnati, Ohio: American Institute of Aeronautics and Astronautics, Jul. 2018. doi: 10.2514/6.2018-4998.

[2] N. A. Pentigill and Zawodny, Nikolas S., "Challenges and Progress in Broadband - Noise Prediction for Small Scale Rotors," in *NASA Acoustics Technical Working Group*, Oct. 2018, p. 28.

[3] N. Hansen, "The CMA Evolution Strategy: A Tutorial." arXiv, Apr. 04, 2016. doi: 10.48550/arXiv.1604.00772.

[4] S. Voß, "Meta-heuristics: The State of the Art," in *Local Search for Planning and Scheduling*, A. Nareyek, Ed., in Lecture Notes in Computer Science, vol. 2148. Berlin, Heidelberg: Springer Berlin Heidelberg, 2001, pp. 1–23. doi: 10.1007/3-540-45612-0_1.

[5] V. T. Ramamoorthy, E. Özcan, A. J. Parkes, A. Sreekumar, L. Jaouen, and F.-X. Bécot, "Comparison of heuristics and metaheuristics for topology optimisation in acoustic porous materials," *J. Acoust. Soc. Am.*, vol. 150, no. 4, pp. 3164–3175, Oct. 2021, doi: 10.1121/10.0006784.

[6] B. Brouard, D. Lafarge, and J. F. Allard, "A general method of modelling sound propagation in layered media," *J. Sound Vib.*, vol. 183, no. 1, pp. 129–142, 1995, doi: https://doi.org/10.1006/jsvi.1995.0243.

[7] "AlphaCell." MATELYS-Research Lab, Vaulx-en-Velin, France, 2023. Accessed: Feb. 28, 2023. [MS Windows, GNU Linux, Mac OS]. Available: https://alphacell.matelys.com/

[8] O. Dazel, J. P. Groby, B. Brouard, and C. Potel, "A stable method to model the acoustic response of multilayered structures," *J Appl Phys.*, vol. 113, no. 083506, 2013, doi: http://dx.doi.org/10.1063/1.4790629.

[9] J.-F. Allard and N. Atalla, *Propagation of sound in porous media: modelling sound absorbing materials*. Wiley, 2009.

[10] J. Magniez, J.-D. Chazot, M. A. Hamdi, and B. Troclet, "A mixed 3D-Shell analytical model for the prediction of sound transmission through sandwich cylinders," *J. Sound Vib.*, vol. 333, no. 19, pp. 4750–4770, Sep. 2014, doi: 10.1016/j.jsv.2014.04.040.

[11] J. Magniez, M. A. Hamdi, J.-D. Chazot, and B. Troclet, "A mixed 'Biot–Shell' analytical model for the prediction of sound transmission through a sandwich cylinder with a poroelastic core," *J. Sound Vib.*, vol. 360, pp. 203–223, Jan. 2016, doi: 10.1016/j.jsv.2015.09.012.

[12] P. Bonfiglio, F. Pompoli, and R. Lionti, "A reduced-order integral formulation to account for the finite size effect of isotropic square panels using the transfer matrix method doi:http://dx.doi.org/10.1121/1.4945717," *J. Acoust. Soc. Am.*, vol. 139, no. 4, pp. 1773–1783, 2016.

[13] N. Hansen, "The CMA Evolution Strategy," *The CMA Evolution Strategy*, 2023. http://www.cmap.polytechnique.fr/~nikolaus.hansen/cmaesintro.html

[14] C. Boutin and F. X. Bécot, "Theory and experiments on poro-acoustics with inner resonators," *Wave Motion*, vol. 54, pp. 76–99, Apr. 2015, doi: 10.1016/j.wavemoti.2014.11.013.

[15] C. Boutin, "Acoustics of porous media with inner resonators," *J. Acoust. Soc. Am.*, vol. 134, no. 6, pp. 4717–4729, 2013, doi: doi:http://dx.doi.org/10.1121/1.4824965.